

Electric Dipole Moments of Impact-Excited He Atoms

A. S. Aynacioglu, S. Heumann, and G. von Oppen

*Institut für Strahlungs- und Kernphysik, Technische Universität Berlin,
D-1000 Berlin 12, Federal Republic of Germany*

(Received 5 December 1989)

We excited helium atoms using 10–20-keV H_2^+ (D_2^+) ion impact and investigated the intensity of the $\lambda(4^3D-2^3P)=447$ -nm line as a function of an electric field -2 kV/cm $\lesssim F \leq +2$ kV/cm applied antiparallel and parallel to the ion beam. The recorded signals were strongly asymmetric with respect to the sign of the electric field. This asymmetry is explained by assuming a coherent excitation of He levels with different angular momenta ($4d, 4f$ and $5f, 5g$). These measurements demonstrate that angular momentum coherences of impact-excited states can also be observed in nonhydrogenic systems.

PACS numbers: 34.50.Fa, 32.80.-t

The state of an atomic target “immediately after a collision” is usually a coherent superposition of stationary states of the atom. Regarding atomic hydrogen, the coherence parameters of collisionally excited superposition states have been investigated experimentally and theoretically in recent years.^{1,2} In particular, angular momentum coherences of hydrogen atoms excited by charge-exchange collisions have been studied by observing the impact radiation as a function of axial and transverse electric fields.³ Owing to the (near) degeneracy of the hydrogenic states with the same n but different l quantum numbers, the collisional interaction time τ_{coll} is several orders of magnitude shorter than the periods of the subsequent atomic evolution and, therefore, the concept of impact-excited states immediately after a collision has a solid foundation.

In this Letter we consider angular momentum coherences of impact-excited helium atoms. Because of the larger energy separations ΔE between levels with different l , the applicability of the concept of transient impact-excited superposition states is less obvious. It is applicable only if

$$\Delta E/\hbar \ll 1/\tau_{\text{coll}}, \quad (1)$$

that is, if the envisaged collisionally excited coherent superposition of eigenstates evolves unperturbed by interactions with the receding collision partner. The appropriate collisional interaction time τ_{coll} may be estimated by considering the evolution of the atomic state in the electric field $F_p = e/4\pi\epsilon_0 R^2$ of the receding ion for which a straight-line trajectory $R(t) = v_p t$ is assumed. Here we are interested in transitions induced to (or from) $n=4$ and $n=5$ states. The corresponding transition matrix elements are at most of the order (using atomic units) $\hbar\omega_1 \approx |\langle nlm | e\mathbf{r} \cdot \mathbf{F}_p | n'l'm' \rangle| \sim n^2/R^2$. Hence, the precession angle φ_τ describing the evolution in a two-state subspace due to the postcollisional interaction⁴ (PCI) after the time τ is at most of the order

$$\varphi_\tau \lesssim \int_\tau^\infty \omega_1(t) dt \lesssim n^2/v_p^2 \tau. \quad (2)$$

This precession is negligible if

$$\tau \gg \tau_{\text{coll}} \approx n^2/v_p^2. \quad (3)$$

Using ions with $v_p^2 \gtrsim 0.1$, the inequality (1) is valid provided $\Delta E \ll 0.1/n^2$.

According to this estimate, it is reasonable to investigate angular momentum coherences of $l \geq 2$ states in HeI. Our experiments concern the coherent excitation of singly excited $1s4d$ and $1s4f$ levels ($\Delta E \approx 210$ GHz h) as well as of the $1s5f$ and $1s5g$ levels ($\Delta E \approx 15$ GHz h). We investigated the impact radiation at $\lambda(1s4d^3D-1s2p^3P)=447$ nm as a function of an electric field -2 kV/cm $\leq F \leq +2$ kV/cm applied parallel and antiparallel to a 10–20-keV H_2^+ (D_2^+) ion beam used for excitation. The experiments were performed using an experimental setup similar to that one described recently.⁵ The H_2^+ or D_2^+ -ion beam was crossed with a He atomic beam effusing from a capillary multichannel plate and directed onto the entrance of a 360-l/s turbomolecular pump. The He-atom density within the target region was estimated at $\sim 10^{13}/\text{cm}^3$. Using a photomultiplier, the impact radiation at various spectral lines selected with interference filters was observed in a direction perpendicular to the ion beam. The ion beam crossed the separately evacuated target chamber through a pair of tubes (diam = 7 mm) used as electric-field electrodes. By applying voltages up to 1 kV with opposite signs, electric fields up to $F \approx 2$ kV/cm were produced in the target region (spacing between the tubes $d=7$ mm) while the electric potential at the center of the target remained unchanged. The voltage applied to the electric-field electrodes did not have any measurable influence on the ion-beam intensity monitored behind the target chamber. In order to avoid intensity changes of the impact radiation due to electron bombardment, care was taken to keep the target region free of secondary electrons. To make sure that spurious effects of the electric fields were reasonably small, we investigated the impact radiation of the $1s3s^3S-1s2p^3P$ transition as a function of the electric field -2 kV/cm $\leq F \leq +2$ kV/cm

cm. Intensity variations no larger than the noise level, i.e., $< 2\%$, were observed.

Quite different results were obtained when the intensity I_{447} of the line $\lambda(4^3D-2^3P)=447$ nm (Fig. 1) was observed. Intensity variations between 10% and 20% were recorded. At the highest projectile velocity (20-keV H_2^+) the intensity decreased monotonically when scanning the electric field from $F = -2$ kV/cm (directed upstream) to $F = +2$ kV/cm. At lower projectile velocities the overall decrease was superimposed by salient structures near $F=0$, changing systematically from a dip at the lowest velocity (10-keV D_2^+), through a dispersion-shaped structure (15-keV D_2^+), to a peak at higher velocities (10-keV H_2^+ , 15-keV H_2^+). D_2^+ measurements at 20 keV yielded about equal results as H_2^+ measurements at 10 keV.

The electric-field dependence of the intensity of the impact radiation, in particular its asymmetry with respect to the sign of the field, indicates a coherent excitation of opposite-parity states.^{3,6} Accordingly, the expectation values of the electric dipole operator are nonzero for the impact-excited states. Of primary importance when investigating the 447-nm line of He atoms in electric fields is the direct excitation of the $4d$ and $4f$ states and the cascade feeding of these states via $5f$ and $5g$ states. In the case of direct excitation the electric-field dependence of I_{447} results from the fact that the $4d$ Stark states acquire $4f$ admixtures and, hence, electric dipole moments at nonzero electric fields. If these moments have the same sign as the moment of the impact-excited states, then I_{447} increases with increasing electric-field strength; otherwise it decreases. The signal structures near $F=0$ can only be explained by taking

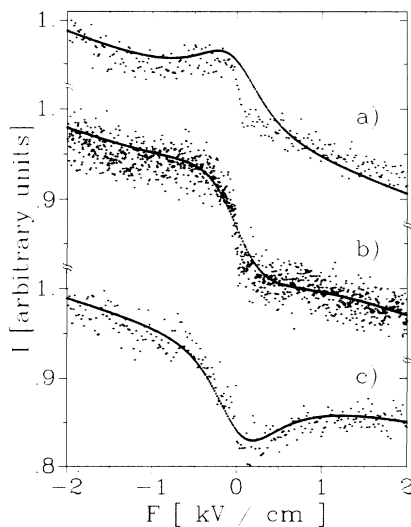


FIG. 1. The intensity I_{447} of the 447-nm line as function of the electric field F after (a) 10-keV H_2^+ , (b) 15-keV D_2^+ , and (c) 10-keV D_2^+ impact. The fitted curves (solid lines) were calculated by using the parameters of Table I.

into account cascade feeding of the $4d$ states. Because of the smaller energy separation of the $5f$ and $5g$ levels, these opposite-parity states are mixed by weaker electric fields. Therefore, the cascade transition rates are changed significantly by the applied electric fields and both the $5f$ and $5g$ Stark substates contribute to the cascade feeding of the $4d$ states.

For a quantitative evaluation of the electric-field dependence we assume the following simplifications: (i) We disregard the influence of the magnetic fine-structure coupling on the evolution of the impact-excited states, and (ii) we presuppose a perfect alignment of the impact-excited states along the ion beam, i.e., that only $m=0$ states are excited. If we do so, we are left with two-state systems. With direct excitation, we have only the $m=0$ states of the $4d$ and $4f$ electron to consider, and with cascade excitation, only the $m=0$ states of the $5f$ and $5g$ electron.

These two-state systems can be considered to be fictitious spin- $\frac{1}{2}$ systems.⁷ Accordingly, the excitation matrices ρ_n describing the impact-excited $n=4$ and $n=5$ states can be characterized by four parameters: $\sigma_n = \text{Tr} \rho_n$ (total excitation cross sections $\sigma_4 = \sigma_{4f} + \sigma_{4d}$ and $\sigma_5 = \sigma_{5g} + \sigma_{5f}$), $\rho_n^x = \text{Tr}(\rho_n \sigma_x) / \sigma_n$ (asymmetry of charge distribution³), $\rho_n^y = \text{Tr}(\rho_n \sigma_y) / \sigma_n$ (asymmetry of current distribution⁸), and $\rho_n^z = \text{Tr}(\rho_n \sigma_z) / \sigma_n$ (relative population difference), where $\sigma = (\sigma_x, \sigma_y, \sigma_z)$ are Pauli's spin matrices. The measured intensity I_{447} depends upon the excitation cross sections

$$\sigma_n^\pm(F) = \langle \psi_n^\pm | \rho_n | \psi_n^\pm \rangle \quad (4)$$

of the normalized eigenstates ψ^\pm of the Stark levels which are completely characterized by the mixing angle ϑ_n defined by $\langle \psi_n^\pm | \sigma | \psi_n^\pm \rangle = \pm (\sin \vartheta_n, 0, \cos \vartheta_n)$. For electric fields $F \lesssim 2$ kV/cm one finds $|\tan \vartheta_4| \lesssim 0.2$, whereas $|\tan \vartheta_5| \lesssim 4$. Because of the small size of the mixing parameter $\tan \vartheta_4$, the decay of the Stark substates of the $4f$ level to the $2p$ level can be disregarded. Then I_{447} is proportional to the occupation of the Stark substates of the $4d$ level because the impact-excited target atoms are within the observation region for their entire lifetime ($\tau \lesssim 200$ ns) and excitation and decay of the eigenstates can be described by rate equations. Regarding direct excitation, one finds

$$\begin{aligned} I_{447}^{\text{dir}} \propto \sigma_4^-(F) &= \frac{1}{2} \sigma_4 (1 - \rho_4^z \cos \vartheta_4 - \rho_4^x \sin \vartheta_4) \\ &\approx \sigma_{4d} - \frac{1}{2} \rho_4^x \sigma_4 \sin \vartheta_4. \end{aligned} \quad (5)$$

However, regarding cascade feeding of the $4d$ state, the variation of the decay rates of the $n=5$ levels with the strength of the field has to be taken into account. Hence, the cascade contributions of the $5f$ and $5g$ Stark states to the population of the $4d$ Stark state are given by

$$I_{447}^{\text{case}} \propto \gamma_5^+ \sigma_5^+ + \gamma_5^- \sigma_5^-, \quad (6)$$

with the branching ratios

$$\gamma_5^- = \frac{A_{4d}^{5f}(1 + \cos\vartheta_5) + (A_{4d}^{5f}A_{4f}^{5g})^{1/2} \sin\vartheta_5 \sin\vartheta_4}{(A_{4d}^{5f} + A_{3d}^{5f} + A_{4f}^{5g}) + (A_{4d}^{5f} + A_{3d}^{5f} - A_{4f}^{5g}) \cos\vartheta_5},$$

$$\gamma_5^+ = \frac{A_{4f}^{5g}(1 - \cos\vartheta_5) - (A_{4d}^{5f}A_{4f}^{5g})^{1/2} \sin\vartheta_5 \sin\vartheta_4}{(A_{4f}^{5g} + A_{4d}^{5f} + A_{3d}^{5f}) + (A_{4f}^{5g} - A_{4d}^{5f} - A_{3d}^{5f}) \cos\vartheta_5},$$

where the $A_{n'l}^{n'l'}$ are the zero-field transition rates.⁹ According to (5) and (6), the observed intensity $I_{447} = I_{447}^{\text{dir}} + I_{447}^{\text{casc}}$ is independent of the ρ_n^y but depends on the charge distribution parameters ρ_n^x , which are related to the expectation values $\langle -ez \rangle_n$ of the electric dipole operator by

$$\langle -ez \rangle_4 = \rho_4^x \langle 4f, 0 | -ez | 4d, 0 \rangle$$

and

$$\langle -ez \rangle_5 = \rho_5^x \langle 5g, 0 | -ez | 5f, 0 \rangle,$$

and on the relative population difference $\rho_5^z = (\sigma_{5g} - \sigma_{5f}) / (\sigma_{5g} + \sigma_{5f})$. (Since ϑ_4 is small, I_{447} is essentially independent of ρ_4^z .)

In spite of the simplifying assumptions made, the intensity variations calculated with (5) and (6) are in overall agreement with the measured signals, if suitable parameters are inserted (see Fig. 1). The general slope of the signals indicates that the dipole moments of the impact-excited states are directed upstream ($\rho_n^x > 0$), i.e., the center of the electron cloud is shifted downstream with respect to the nucleus. The shape of the central signal structure near $F=0$ depends on the ratio ρ_5^x / ρ_5^z . One finds $\rho_5^z > 0$ at the lowest projectile velocity and $\rho_5^z < 0$ at higher velocities (Table I).

Though the essential features of the observed signals are reproduced by the simplifying two-state calculations, it is not surprising that there are some unexplained minor discrepancies between the experimental signals and the calculated curves. Cascade feedings via high- l levels with $n > 5$ may significantly influence the shape of the signals near $F=0$. At higher electric fields, the decoupling of spin and orbital motion in the 4^3D states and, in particular, the demixing of singlet and triplet $5f$ and $5g$ states due to the (above completely neglected) interaction of these states with the $5d$ configuration⁵ are expected to affect the electric-field dependence of I_{447} .

TABLE I. Parameters used for fitting the experimental signals (Fig. 1) with the functions defined in (5) and (6).

Projectile velocity (a.u.)	ρ_4^x	ρ_5^x	ρ_5^z	σ_5 / σ_4
0.32 (10-keV D_2^+)	0.29	0.19	0.05	1
0.39 (15-keV D_2^+)	0.50	0.45	-0.21	1
0.45 (10-keV H_2^+)	0.42	0.23	-0.66	0.5
0.55 (15-keV H_2^+)	0.29	0.10	-0.69	0.25
0.63 (20-keV H_2^+)	0.27	0

Here we used H_2^+ (D_2^+) ions as projectiles, allowing excitation of He singlet as well as triplet states. Therefore, it is justified to disregard the S - T demixing in a first analysis. A different situation is encountered when H^+ or H_3^+ ions are used for excitation. Here, according to Wigner's spin conservation rule, singlet states are excited more selectively. Since the demixing depends on F^2 , it is independent of the sign of F . Usually, both S - T demixing and angular momentum coherences of the impact-excited states affect the electric-field dependence of the intensity of the 447-nm line and more complicated signal structures are observed.¹⁰ Finally, regarding the restriction of our analysis to $m=0$ states, we emphasize that polarization measurements indicated that indeed the low- $|m|$ states of the high- l levels of helium are preferably populated by ion-impact excitation.^{5,10}

Our experimental results demonstrate that, besides collisionally excited hydrogen atoms, impact-excited states of helium can also have large electric dipole moments. In the hydrogen experiments^{1,3} charge-exchange collisions have been investigated. Here we considered direct excitation. In both cases total (i.e., angle integrated) cross sections were measured. Therefore, only the electric dipole component parallel to the ion beam is monitored. The fact that these dipole components are large (and do not average out by integration over the impact parameter) indicates that the final phase of the collision process where the axis of the collision system is almost aligned with the ion beam is essential for the formation of the electric dipole moment. A similar conclusion can be drawn from magnetic depolarization measurements^{5,10} which indicate a significant alignment, i.e., the preferential excitation of the $m=0$ states of high- l levels of He by hydrogen-ion impact. It is tempting to explain the alignment of the excited atoms along the beam axis by referring to the electrostatic postcollisional interaction.⁵ However, regarding impact-excited states of hydrogen, Burgdörfer and Dube⁴ have shown that PCI does not give rise to the formation of electric dipole moments. Therefore, it may be worthwhile to conclude by emphasizing some other aspects of the final phase of the collision. Beside explaining the alignment of the excited atom, they also enlighten another somewhat surprising result of our measurements: the very fact that high- l levels up to $l=n-1$ are effectively populated at medium ion velocities.

After the excitation of $n=2$ states during the close encounter, the molecular system $(H_2He)^+$ transforms into the separated-atom limit during the final phase of the collision. Though the diabatic molecular-orbital model can be applied to the close encounter,¹¹ its application is much less justified when considering the final phase since the excited electrons move more slowly. Accordingly, one expects that the electron cloud which is centered at the center of mass during the close encounter lags behind the separating atoms; i.e., after the collision the centers of the electron clouds of the separated atoms are some-

what shifted from the sites of the respective nuclei, towards the center of mass of the collision system. This shift implies the formation of electric dipole moments as well as transitions to higher- n and higher- l states. A decisive feature of this final-phase evolution of the collision system is the fact that it not only takes place within the Hilbert space of nearly degenerate states (with the same n , as assumed in Ref. 4), but also involves transitions (e.g., $2p \rightarrow 3d \rightarrow 4f \dots$) between different n states which can be induced by an effective operator describing the translational shift of the electron cloud.¹² We emphasize that according to these ideas, the formation of electric dipole moments is not due to the attractive force of the receding ion but due to the inertia of the electron cloud. Therefore, large electric dipole moments of impact-excited states should also be observable in atom-atom collisions.

The authors are grateful to D. Kaiser and Y. Kriescher for their stimulating discussions. This work has been supported by the Deutsche Forschungsgemeinschaft.

¹R. DeSerio *et al.*, Phys. Rev. A **37**, 4111 (1988), and references therein.

²A. Jain, C. D. Lin, and W. Fritsch, J. Phys. B **21**, 1545 (1988), and references therein.

³C. C. Havener *et al.*, Phys. Rev. A **33**, 276 (1986); J. R. Ashburn *et al.*, Phys. Rev. A **40**, 4885 (1989).

⁴J. Burgdörfer and L. J. Dubé, Phys. Rev. Lett. **52**, 2225 (1984).

⁵A. S. Aynacioglu, G. v. Oppen, and R. Müller, Z. Phys. D **6**, 155 (1987).

⁶T. G. Eck, Phys. Rev. Lett. **31**, 270 (1973).

⁷C. Cohen-Tannoudji, B. Diu, and F. Laloë, *Quantum Mechanics* (Wiley, New York, 1977), Vol. I.

⁸C. C. Havener *et al.*, Phys. Rev. Lett. **53**, 1049 (1984).

⁹W. L. Wiese, M. W. Smith, and B. M. Glennon, *Atomic Transition Probabilities*, National Standard Reference Data Series—4 (U.S. GPO, Washington, DC, 1966), Vol. I.

¹⁰A. S. Aynacioglu, S. Heumann, and A. H. Meissner (unpublished).

¹¹A. Russek and R. J. Furlan, Phys. Rev. A **39**, 5034 (1989).

¹²D. R. Bates and R. McCarroll, Proc. Roy. Soc. London A **245**, 175 (1958).